

UCLA

UCLA Previously Published Works

Title

Three-repeat and four-repeat tau isoforms form different oligomers

Permalink

<https://escholarship.org/uc/item/98h1w8br>

Journal

Protein Science, 31(3)

ISSN

0961-8368

Authors

Shahpasand-Kroner, Hedieh
Portillo, Jennifer
Lantz, Carter
et al.

Publication Date


2022-03-01

DOI

10.1002/pro.4257

Peer reviewed

Three-repeat and four-repeat tau isoforms form different oligomers

Hedieh Shahpasand-Kroner¹ | Jennifer Portillo¹ | Carter Lantz² |
Paul M. Seidler³ | Natalie Sarafian¹ | Joseph A. Loo^{2,4,5} | Gal Bitan^{1,4,6} 

¹Department of Neurology, David Geffen School of Medicine, University of California, Los Angeles, California, USA

²Department of Chemistry and Biochemistry, University of California, Los Angeles, California, USA

³Department of Pharmacology and Pharmaceutical Sciences, University of Southern California School of Pharmacy, Los Angeles, California, USA

⁴Molecular Biology Institute, University of California, Los Angeles, California, USA

⁵Department of Biological Chemistry, University of California, Los Angeles, California, USA

⁶Brain Research Institute, University of California, Los Angeles, California, USA

Correspondence

Gal Bitan, Department of Neurology, David Geffen School of Medicine at UCLA, Gordon Neuroscience Research Building, Room 451, 635 Charles E. Young Drive South, Los Angeles, CA 90095-7334, USA.
Email: gbitan@mednet.ucla.edu

Funding information

Department of Energy, Labor and Economic Growth, Grant/Award Number: DE-FC02-02ER63421; National Institute on Aging, Grant/Award Numbers: R01AG050721, RF1AG054000, RF1AG054000-01A1S1; National Institutes of Health, Grant/Award Numbers: GM007185, R01GM103479, S10 OD018504

Abstract

Different tauopathies are characterized by the isoform-specific composition of the aggregates found in the brain and by structurally distinct tau strains. Although tau oligomers have been implicated as important neurotoxic species, little is known about how the primary structures of the six human tau isoforms affect tau oligomerization because the oligomers are metastable and difficult to analyze. To address this knowledge gap, here, we analyzed the initial oligomers formed by the six tau isoforms in the absence of posttranslational modifications or other manipulations using dot blots probed by an oligomer-specific antibody, native-PAGE/western blots, photo-induced cross-linking of unmodified proteins, mass-spectrometry, and ion-mobility spectroscopy. We found that under these conditions, three-repeat (3R) isoforms are more prone than four-repeat (4R) isoforms to form oligomers. We also tested whether known inhibitors of tau aggregation affect its oligomerization using three small molecules representing different classes of tau aggregation inhibitors, Methylene Blue (MB), the molecular tweezer CLR01, and the all-D peptide TLKIVW, for their ability to inhibit or modulate the oligomerization of the six tau isoforms. Unlike their reported inhibitory effect on tau fibrillation, the inhibitors had little or no effect on the initial oligomerization. Our study provides novel insight into the primary–quaternary structure relationship of human tau and suggests that 3R-tau oligomers may be an important target for future development of compounds targeting pathological tau assemblies.

KEYWORDS

inhibitor, oligomerization, tau isoforms, tauopathies

1 | INTRODUCTION

The human microtubule-associated protein tau is encoded by a single gene residing on chromosome 17, which is translated into six isoforms as a result of

alternative mRNA splicing of exons 2, 3, and 10 in the central nervous system.^{1,2} The six isoforms differ by the absence or presence of 1 or 2 N-terminal inserts (0N, 1N, or 2N), and either three (3R) or four (4R) 31- or 32-amino acid repeats in the microtubule-binding

domain. The expression of tau isoforms is regulated developmentally. All six isoforms are expressed in the adult human brain,¹ whereas only 0N3R, the shortest tau isoform, is expressed in the fetal brain.³ Tau is expressed predominantly in neurons, but it is also found at lower expression levels in other cell types and in various organs, including heart, kidney, lung, and liver.^{4,5} In neurons, tau is found primarily in axons and to a lower extent in dendrites, where it regulates microtubule assembly and maintenance, neurite outgrowth, axonal elongation, and axonal transport.^{6–8}

Approximately equal amounts of 3R and 4R tau isoforms are present in the adult human brain, yet 2N forms are underrepresented compared to 0N and 1N isoforms. The regulation of tau-isoform expression varies in different brain regions. For example, 0N3R tau is expressed at lower levels in the cerebellum compared to other brain regions and 4R tau isoforms are elevated in the globus pallidus.^{9–11} Under pathological conditions, including neurodegenerative diseases and brain injury, tau dissociates from the microtubules and self-assembles first into water-soluble oligomers, and later into insoluble fibrillar aggregates.¹² These processes are associated with abnormal posttranslational modifications of tau, of which hyperphosphorylation has been studied the most, yet the details of these events, including their temporal order and spatial distribution, are yet to be deciphered.

Over 20 neurodegenerative diseases known as tauopathies are associated with aberrant self-assembly of tau into oligomers and fibrils.¹³ Based on the tau isoforms found in brain deposits post-mortem, tauopathies are divided into three groups, including 3R tauopathies, such as Pick's disease (PiD); 4R tauopathies, including progressive supranuclear palsy (PSP), corticobasal syndrome (CBS), argyrophilic grain disease (AGD), and globular glial tauopathy (GGT); and 3R + 4R tauopathies such as Alzheimer's disease (AD), frontotemporal dementia with parkinsonism linked to chromosome 17 (FTDP-17), and chronic traumatic encephalopathy (CTE).^{13,14} Each disease is characterized by pathogenic tau inclusions, such as neurofibrillary tangles (NFT) in AD, Pick bodies in PiD, and mixed neuronal and glial inclusions in PSP, CBS, and CTE.^{15,16} Different tauopathy models have been generated for studying the pathology of 3R and 4R tau isoforms related to the various tauopathies, yet the distinct pathogenic properties of the different tau isoforms are still an active area of research. Studies in transgenic drosophila models of tauopathy have suggested that accumulation of either 0N3R and 0N4R human tau isoforms caused functional deficits and that 0N3R-tau accumulation contributed

more to failure in signal transduction compared to 0N4R-tau.^{17,18} To date, to the best of our knowledge, no study has compared directly the initial oligomerization propensity of all six tau isoforms.

Unlike most amyloidogenic proteins, unmodified tau does not aggregate spontaneously. Tau aggregation can be induced in the presence of polyanions, such as nucleic acids, acidic peptides, heparin, or arachidonic acid, or by introducing covalent posttranslational modifications, such as phosphorylation, *in vitro*.^{19–21} Arachidonic acid- and heparin-induced tau filaments of different human tau isoforms have shown distinct assembly properties of each isoform.^{19,20} Heparin-induced 2N4R-tau fibrils consisted of a mixture of ≥ 4 conformations, whereas heparin-induced 2N3R-tau filaments primarily adopted a single conformation.²⁰ Arachidonic acid-induced aggregation of tau suggested that the N-terminal inserts might facilitate tau oligomerization. Thus, arachidonic acid-induced 0N tau aggregation resulted in small, globular oligomers that did not elongate into straight filaments (SFs) or paired helical filaments (PHFs) when compared to other tau isoforms. 1N3R and 2N3R tau isoforms formed PHFs readily when induced to aggregate by arachidonic acid, in contrast to 4R tau isoforms, which formed PHFs less frequently.¹⁹

In the past two decades, most studies have focused on understanding the pathology of insoluble, fibrillar tau aggregates in different tauopathies. However, elevation of oligomeric tau has been reported in patients with AD prior to formation of NFT pathology, suggesting that an increase in tau oligomers might be an early pathologic event in AD.²² Recent studies have shown that neuronal loss and cell death occurred in different tauopathy models before tau-fibril formation suggesting that tau oligomers were the main neurotoxic species.^{23–34} In support of this hypothesis, administration of recombinant tau oligomers into the hippocampus of wild-type mice resulted in immediate memory impairment.²⁵ Direct comparison between tau oligomers and tau fibrils applied extracellularly to SH-SY5Y human neuroblastoma cells found that the oligomers were 60% more neurotoxic.³⁵ Despite recent studies characterizing tau oligomerization, the question how the primary structure of human tau isoforms affects the oligomerization is yet unanswered. To address this question, here we analyzed the initial oligomers formed by the six isoforms in isolation or in a mixture reflecting their physiologic composition using several biochemical and biophysical methods. We also tested known inhibitors of tau fibrillation representing different chemical classes for their ability to affect tau oligomerization.

2 | RESULTS

2.1 | 3R-tau isoforms show a higher reactivity than 4R-tau isoforms with the anti-tau-oligomer antibody TOC1

Our goal in this study was to examine whether oligomers exist in unmodified human tau and if differences exist among the six isoforms, without posttranslational modifications or any other manipulations. We envisioned the study to serve as a baseline for future systematic characterization of posttranslationally modified tau proteins and of variants containing disease-associated sequence variations. To study the oligomerization propensity of different tau isoforms, the purified, recombinant proteins were analyzed first using dot blots probed with antibody Tau Oligomeric specific Complex-1 (TOC1)³⁶ (Figure 1a),

one of several antibodies reported previously to label tau oligomers.^{27,29,37} In initial experiment, we also tried to use antibodies TOMA³⁸ and T22.²⁷ Despite the successful demonstration of using these antibodies by other groups, in our hands, their signal was low and inconsistent compared with TOC1. Therefore, we used TOC1 in all subsequent experiments.

To validate equal protein loading, we probed the same membranes also with the anti-human tau monoclonal antibody (mAb) HT7 (Figure 1a, bottom row). The HT7 reactivity of all tau isoforms was similar, confirming loading equal amounts of the tau isoforms. All the isoforms were found to be TOC1-reactive, yet the signal intensity varied among them (Figure 1a). To quantify the differences, we used densitometry and normalized the intensity of TOC1-reactive dots to the densitometric value of total tau. The analysis showed

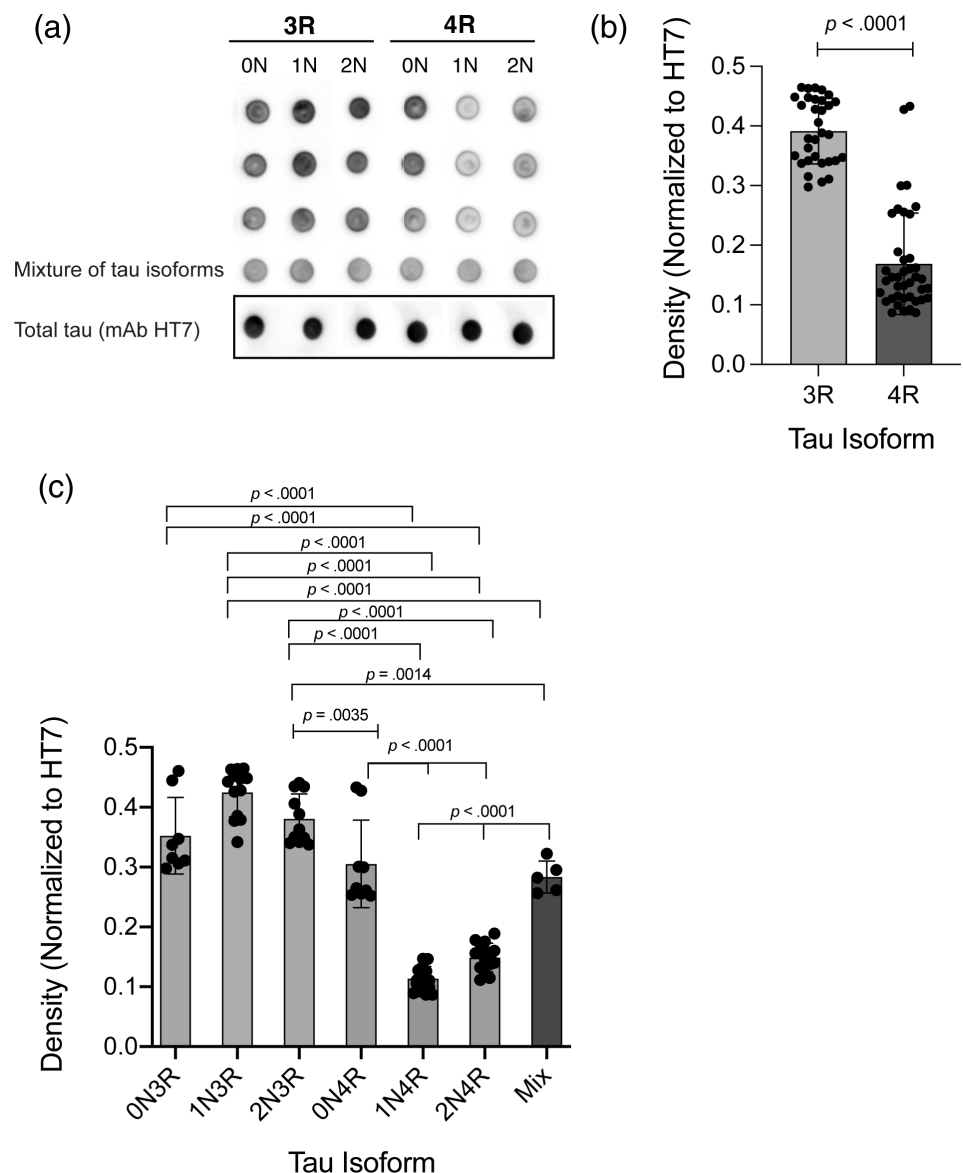


FIGURE 1 Dot-blot analysis of tau isoforms. (a) Each tau isoform was spotted on a nitrocellulose membrane in triplicates and probed with antibody TOC1. (b) A plot of the average densitometric intensity of 3R versus 4R isoforms. The p -value was calculated using an unpaired Student's t -test. (c) A plot of the densitometric intensity of each isoform. Each bar represents an average of three independent experiments, each with at least three technical replicates. The p values were calculated by a one-way ANOVA with Bartlett's test for multiple comparisons and are shown only where $p < .05$

that 3R-tau isoforms had significantly higher TOC1 reactivity compared to 4R-tau isoforms (Figure 1b, $p < .0001$). Comparing each of the individual isoforms showed that 1N3R-tau (normalized densitometric value 0.42 ± 0.04) was the most reactive isoform, though the differences between this isoform and the two other 3R isoforms, 0N3R-tau (0.35 ± 0.06) and 2N3R-tau (0.38 ± 0.04) did not differ significantly (Figure 1c). Among the 4R-tau isoforms, the reactivity of 0N4R-tau (0.30 ± 0.07) was more than twice those of 1N4R-tau (0.11 ± 0.02) or 2N4R-tau (0.14 ± 0.02). The data demonstrated that the absence or presence of the second repeat in the microtubule-binding domain was the main determinant of TOC1 reactivity and that in the context of 4R-, but not 3R-tau, the presence of one N-terminal insert reduced the formation of TOC1-reactive oligomers by $\geq 50\%$, whereas the addition of the second N-terminal insert had little effect on the reactivity.

Next, we asked whether the presence of other isoforms might affect the oligomerization tendency of tau compared to each isoform in isolation. In the adult human brain, the proportion of 3R and 4R tau isoforms are roughly equal and 0N, 1N, and 2N comprise $\sim 37\%$, $\sim 54\%$, and $\sim 9\%$ of total tau, respectively.³⁹ Thus, we tested whether the TOC1-reactivity of a mixture of all the isoforms in these proportions would simply reflect the oligomerization of each isoform or would suggest cooperativity or inhibition of oligomerization. Based on the experimental results of each individual isoform, the weighted average normalized density of the mixture was calculated to be 0.29. The experimental densitometric values measured for the mixture, 0.28 ± 0.03 , suggested that mixing the tau isoforms did not lead to cooperativity or inhibition, but rather reflected simply the TOC1 reactivity for each individual isoform.

2.2 | 3R-tau isoforms form abundant dimers

To investigate the contribution of individual oligomers to the TOC1 reactivity in the dot blots, we analyzed each tau isoform using native polyacrylamide gel electrophoresis (native-PAGE) followed by western blots probed with antibodies TOC1 (Figure S1) and HT7 (Figure 2). Previous studies have suggested that dimerization of 2N4R-tau yields two forms of tau assembly—cysteine-dependent and cysteine-independent dimers, both of which are involved in tau oligomerization, although with different kinetics.⁴⁰ Although we used DTT in our preparation of the tau proteins, DTT was removed before the final step and the proteins were kept in the absence

of DTT before testing their oligomerization state. As a precaution, to test whether oxidation and covalent dimerization might contribute to the observed oligomer size distribution, we analyzed each isoform both in the absence (Figure 2a) and in the presence (Figure 2b) of DTT. Our analysis showed that there were no meaningful differences in the oligomer size distributions between these conditions (Figure 2c–h), suggesting that the oligomers we detected in these experiments were cysteine-independent.

Probing with HT7 showed gel bands ranging from monomer up to at least a putative tetramer and in two cases, up to a putative hexamer (Figure 2a). 0N (Figure 2c) and 1N (Figure 2d) 3R tau isoforms showed bands up to a putative pentamer, whereas the highest band observed for the 2N3R isoform was a tetramer (Figure 3e). All 3R isoforms showed prominent putative dimer bands, which were highest for 1N3R, corresponding to the highest reactivity of TOC1 with this isoform in the dot blots among all six isoforms. Interestingly, 1N3R-tau stood out among the 3R isoform in that the dimer abundance of this isoform was nearly three times higher than the monomer abundance, suggesting strong stabilization of the dimer compared to 0N3R- or 2N3R-tau. In contrast, the monomer was the most abundant band of all the 4R tau isoforms. 0N4R (Figure 2f) showed bands up to a putative pentamer whereas the highest observed oligomers of 1N (Figure 2g) and 2N (Figure 2h) was a hexamer. The monomer abundance of 1N4R-tau was substantially higher and the dimer abundance slightly higher than those of 0N4R- or 2N4R-tau, whereas the abundance of higher-order oligomers of the latter two isoforms was greater than that of 1N4R-tau. Together with the results for the 3R isoforms, these observations suggested that the presence of the sequence corresponding to exon 2 in the N-terminus might contribute to stabilizing the dimer.

To test whether the observed oligomers, particularly the dimers, contributed to the TOC1 reactivity observed in the dot blots (Figure 1), each membrane was probed first with TOC1 before stripping and re-probing with HT7. Surprisingly, no reactivity at all was observed with TOC1 (Figure S1). Potential explanations for this observation are that the higher reactivity of 3R isoforms found in the dot blots probed with TOC1 did not correlate with the abundant tau dimers we detected in 3R tau isoforms using antibody HT7 in these native-PAGE/western blots, that TOC1 does not react with the small oligomers we detected in the native-PAGE/western blots or, more likely, that the fractionation process itself, though gentler than SDS-PAGE, disrupted the TOC1 epitope.

2.3 | 3R-tau isoforms form more abundant cross-linked high molecular weight oligomers than 4R-tau isoforms

In addition to the dot blots and native-PAGE/western blots, to test whether chemical cross-linking might offer additional insight into the oligomer-size distribution of

different tau isoforms, we employed photo-induced cross-linking of unmodified proteins (PICUP),^{41,42} a method used previously to study the oligomerization of multiple amyloidogenic proteins.^{42–44} In this method, photo-activation leads to formation of radicals, resulting in “zero-length” cross-links directly between polypeptide chains without a linker moiety, primarily among Tyr

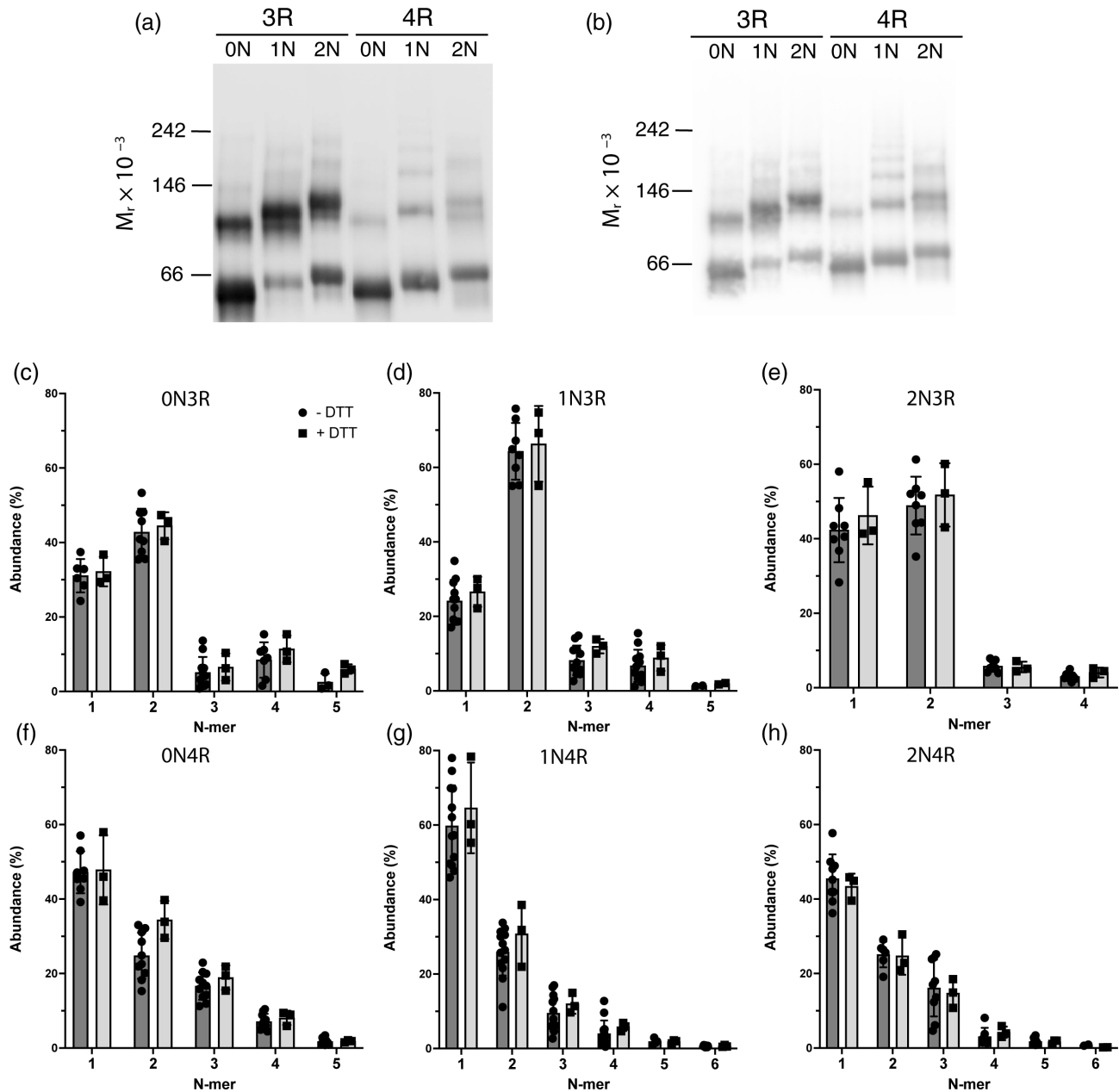


FIGURE 2 Native-PAGE/western blot analysis of tau isoforms. (a) Native-PAGE fractionation of 500 ng of each tau isoform followed by western blotting probed with mAb HT7. Molecular weight markers are shown on the left. The gel is an example of one of six independent experiments. (b) Native-PAGE fractionation of 500 ng of each tau isoform treated with DTT followed by western blotting probed with mAb HT7. The gel is an example of one of three independent experiments. Molecular weight markers are shown on the left. C-H) Quantification of the abundance of each oligomer species (N-mer) for each tau isoform by densitometry. The key in panel (c) applies also to panels (d)–(h). The data are shown as mean \pm SD. Disagreement between the apparent abundance of individual bands in panels (a) or (b) and the quantification results reflects the level of variability in the experimental system

and/or Trp residues.⁴⁵ A set of experiments was carried out first to optimize the protein-to-Ru(Bpy) ratio, while keeping the Ru(Bpy) to APS ratio at 1:20, as recommended.⁴⁶ This optimization step showed that 10 μ M tau and a tau:Ru(Bpy) ratio of 1:4, respectively, resulted

in efficient cross-linking and therefore these conditions were applied to all subsequent PICUP experiments. In all cases, the uncross-linked protein was used as a control. Thanks to the high sensitivity of silver-staining, low-abundance impurities were apparent below the monomer

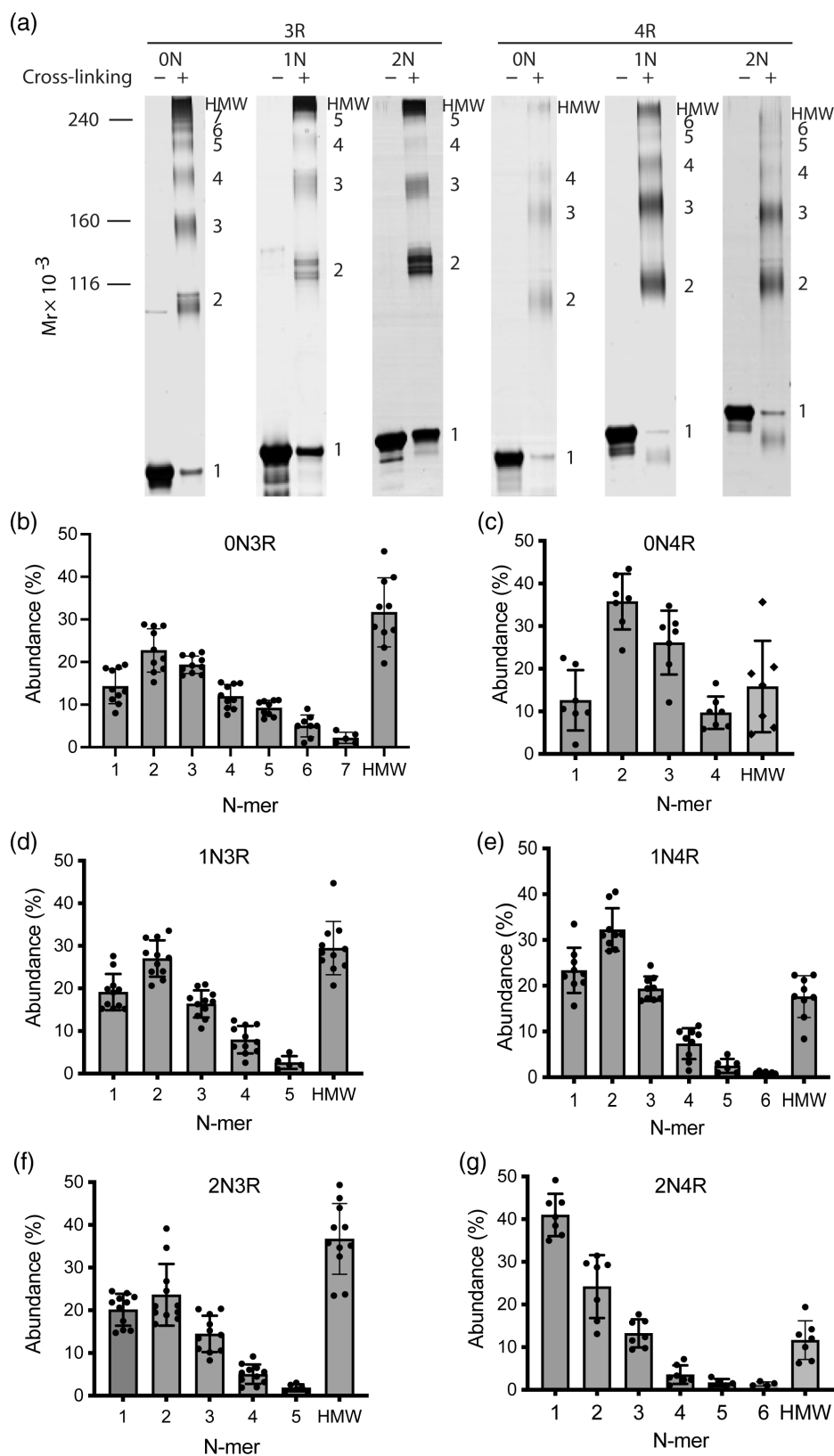


FIGURE 3 PICUP analysis of the six tau isoforms. (a) Representative gels showing cross-linked (+) and non-crosslinked (-) tau isoforms fractionated by SDS-PAGE and silver-stained. The putative oligomer order is noted on the right of each band. The bands below the monomers are either impurities or degradation products. Positions of molecular weight markers are shown on the left. (b-g) The abundance of each band was quantified densitometrically and normalized to the entire lane. Each bar represents an average of three independent experiments, each with at least three technical replicates

band, which decreased in abundance after cross-linking, likely due to degradation under the vigorous radical reaction that yields the polypeptide cross-linking.

Following cross-linking, the oligomer-size distribution was analyzed by SDS-PAGE and silver staining (Figure 3a). The distributions comprised individual bands, in which depending on the isoform, the highest individual oligomer was between a tetramer and a heptamer, and a smear was observed above those bands, in which individual oligomers could not be resolved. We classified this band as high-molecular-weight (HMW) oligomers and quantified it as one entity. The abundance of the HMW oligomers was the most prominent difference between 3R isoforms (Figure 3b,d,f), for which the abundance was 30–40%, and 4R isoforms (Figure 3c,e,g), for which the HMW band abundance was <20%.

The oligomer size distribution of 3R-tau isoforms showed oligomers ranging from dimer through heptamer for 0N3R (Figure 3b) and from dimer through pentamer for 1N3R (Figure 3d) and 2N3R (Figure 3f). PICUP analysis of 0N4R resulted in a size distribution ranging from dimer to tetramer (Figure 3c), whereas the size distribution of 1N4R (Figure 3e) and 2N4R (Figure 3g) cross-linked oligomers displayed bands ranging from dimer to hexamer. Densitometric analysis showed both similarities and differences among the tau isoforms (Figure S2). 3R tau isoforms had similar distributions, suggesting that the N-terminal sequences coded by exons 2 and 3, which do not contain Tyr or Trp, did not contribute meaningfully to the cross-linking. Interestingly, despite the absence of these reactive residues in them, the absence or presence of exon 2- and 3-encoded sequences had a considerable impact on the oligomer size distributions of 4R isoforms, suggesting an interaction between the N-terminus and the repeat domain in these isoforms. Thus, whereas the distribution of 1N4R-tau resembled that of 1N3R-tau, in 0N4R-tau the dimer (36%) and trimer (26%) were more prominent than in all other isoforms and no oligomers above a tetramer were observed, suggesting stabilization of dimers and trimers of this isoform. The opposite picture was observed in 2N4R-tau, the only isoform in which the dimer abundance was lower than that of the monomer, suggesting destabilization of dimers and higher-order oligomers of this isoform. Some cross-linked oligomers appeared split into two or more bands, suggesting stabilization of different conformers.

2.4 | Mass spectrometry and ion-mobility analysis of tau isoforms

As important complementary methods, mass spectrometry (MS) and ion-mobility-coupled mass spectrometry

(IM-MS) were used to analyze the oligomer abundance of each tau isoform. Though these methods, which analyze the protein in the gas phase, are not directly comparable to solution-phase methods, they provide useful information that can be correlated with the results obtained in solution and have been used in many cases for similar analyses of amyloidogenic proteins.^{47–50} Our analysis showed monomers and dimers, but not higher oligomers, likely because they are too large to be transferred in a stable form into the gas phase. Although oligomers have been reported before for tau-derived peptides or fragments,^{51–56} to the best of our knowledge, previous IM-MS studies of full-length tau did not report oligomers^{49,57–59} and this is the first such report. We used the dimer abundance to compare among the tau isoforms and to examine to what extent the data correlated with the solution-phase analyses (Figure S2).

The dimer abundance of 3R isoforms showed a slight increase in the order 0N (0.49%), 1N (0.56%), 2N (0.88%; Figure 4a), though these differences were statistically insignificant ($p > .2$). In contrast, the dimer abundance of 0N4R-tau, 2.71%, was substantially higher than those of all the other isoforms and was significantly higher ($p < .0001$, Figure 4a, gray bars only) than those of 1N4R-tau (0.43%) or 2N4R-tau (0.85%) and from all the 3R isoforms. IM-MS analysis of the isoforms showed a somewhat higher dimer abundance than the MS spectra for all the isoforms (Figure 4b), likely reflecting the higher sensitivity of the method for detecting oligomers compared to MS. The measurements supported the observation that the dimer abundance of 0N4R-tau was the highest among the six isoforms, yet due to higher variability of these measurements, the differences were not statistically meaningful ($p > .17$, Figure 4b, gray bars only).

Comparing the dimer abundance measured by the four methods we used showed that for all isoforms, the abundance measured using the solution-state techniques, native-PAGE and PICUP/SDS-PAGE was substantially higher than by the gas-phase methods, MS and IM-MS. Nonetheless, plotting the data using two y-axes (Figure S2) clearly showed a different pattern for the 3R compared to the 4R isoforms. All the 3R isoforms followed the same behavior, showing higher dimer abundance by native-PAGE compared to PICUP, whereas the abundance for 4R isoforms was similar between the two methods or higher in PICUP. The 0N4R, in particular, displayed a unique pattern, which was more consistent among the different techniques, emphasizing that dimers of this isoform might be particularly stabilized compared to the other isoforms.

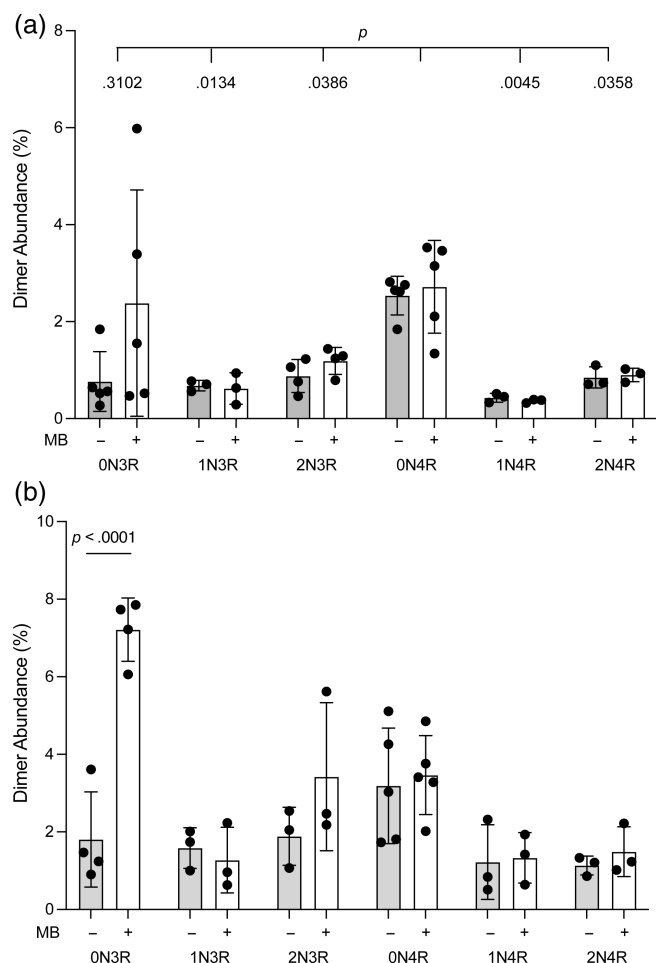


FIGURE 4 Relative abundance of dimers in MS and IM-MS in the absence (gray bars) or presence (white bars) of MB. (a) Dimer abundance is estimated based on MS peak intensity. The data are presented as mean \pm SD. The p values were calculated by a two-way ANOVA for multiple comparisons and are shown only for comparison of each isoform with 0N4R-tau. (b) Dimer abundance extracted from IM-MS mobiligrams. The data are presented as mean \pm SD. The p values were calculated by a two-way ANOVA for multiple comparisons. $p > .05$ values are not shown

2.5 | Effect of aggregation inhibitors on tau oligomerization

Next, we asked whether and how known aggregation inhibitors might affect tau oligomerization. Several classes of compounds have been tested as tau aggregation inhibitors including small molecules and peptides.^{60–65} MB was shown to inhibit tau aggregation and reached phase-3 clinical trials, though unfortunately, it failed to achieve a significant therapeutic effect,^{64,65} possibly because it targets only tau and not A β .⁶⁶ In contrast, the molecular tweezer CLR01 was found to inhibit both A β and tau aggregation,^{67,68} A β toxicity,^{67,69,70} and tau seeding in cell culture,⁶⁸ and both proteins' in vivo

pathology.^{62,70} The tau-specific aggregation inhibitor-peptide, D-TKLIVW, has been reported to inhibit tau aggregation effectively in vitro,^{71,72} and has not been tested in vivo.

To test if MB, CLR01, and/or D-TLKIVW, which act by different mechanisms of action, modulate initial tau oligomerization, we added each inhibitor to each tau isoform and analyzed the effect of the inhibitors using TOC1-probed dot blots, native-PAGE/western blot probed with HT7, MS, and IM-MS. The protein to inhibitor ratio was 1:10 in all cases. As PICUP cross-linking occurs mostly through Trp and Tyr residues, D-TLKIVW was expected to interfere with this chemistry and therefore we did not include PICUP in the analysis of the potential inhibitors.

For the dot-blot analysis, 10 μ M of each tau isoform were used and 500 ng of the protein in the absence or presence of each inhibitor were spotted on the membrane (Figure 5a–c). Having established that loading of the dots was consistent in all cases, in these experiments, we did not probe the membranes with HT7 and therefore the quantitative comparison here is of the absolute densitometric values. The analysis showed that the TOC1 reactivity of 3R-, but not 4R-tau isoforms decreased in the presence of MB (Figure 5a, d). The densitometric signal of 0N3R decreased from $8,108 \pm 607$ in the absence of MB to $6,197 \pm 1854$ in the presence of the compound (24% inhibition, $p = .063$). The average value in the presence of MB seemed to be affected by one outstanding high-value data point (Figure 4d). When this data point was excluded, the inhibitory effect increased to 30% ($p = .003$). A highly similar inhibition was found for the 1N3R and 2N3R isoforms. The densitometric signal for the former decreased from $8,389 \pm 1,453$ in the absence of MB to $5,912 \pm 1,127$ in the presence of MB (30% inhibition, $p = .003$), whereas for the latter the signal decreased from $6,659 \pm 1,471$ to $4,820 \pm 703$ (28% inhibition, $p = .03$).

Neither CLR01 nor D-TLKIVW affected the reactivity of TOC1 to any of the tau isoforms compared to the same isoforms analyzed in the absence of the inhibitor (Figure 4b,c,e,f). Previously, we reported that CLR01 inhibited tau oligomerization and tau-seeding in the P301S mouse model of tauopathy,⁶² yet in that case, the oligomers formed in vivo likely were different from those analyzed here. In addition, in vivo, an important component of CLR01's mechanism of action is facilitating lysosomal degradation,⁷³ which cannot be assessed in an in vitro system, such as the one used here.

To assess whether specific tau oligomers might have been inhibited by MB, we analyzed each isoform in the absence or presence of MB using native-PAGE followed by western blots probed with mAb HT7. We also tested

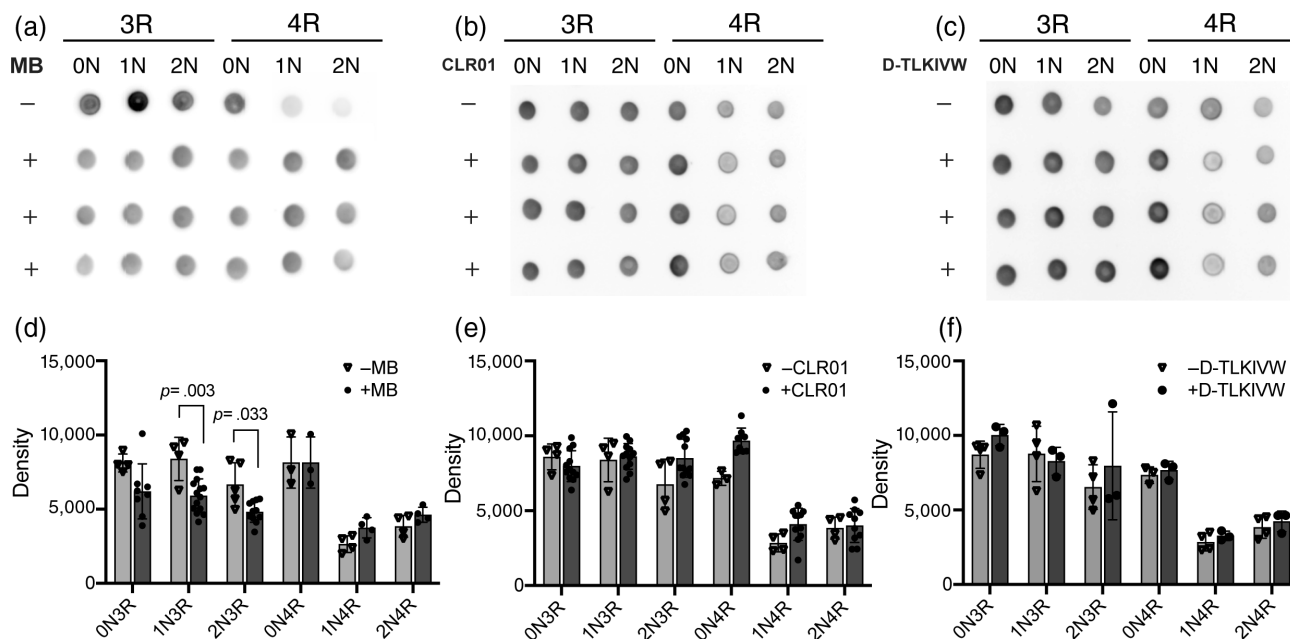


FIGURE 5 Dot-blot analysis of tau isoforms in the absence or presence of MB, CLR01, or D-TLKIVW. (a–c) Dot blot analysis of tau isoforms, 500 ng/spot, in the absence (–) or presence (+) of MB (a), CLR01 (b), or D-TLKIVW. Then, 100 μ M of each inhibitor were added to 10 μ M of each tau isoform and the mixture was spotted immediately on a nitrocellulose membrane in triplicates and probed with TOC1. (d–f) Densitometric analysis of the dot blots. Each bar represents an average of three independent experiments, each with at least three technical replicates. The p values were calculated by a two-way ANOVA. Only p values $<.05$ are shown

the other two inhibitors to check if they might shift the oligomer size distribution in a way that TOC1 dot-blot could not reveal (Figure S3). In contrast to the $\sim 30\%$ reduction in TOC1 reactivity with 3R isoforms in dot blots the presence of MB, we did not observe any modulation of the oligomer size distribution of any tau isoform by MB, CLR01, or D-TLKIVW in the native-PAGE/western blots probed with mAb HT7 (Figure S3).

We also tested the effect of MB on the dimer abundance of each isoform by and IM-MS. The MS analysis indicated a ~ 3 -fold increase in dimer abundance of 0N3R-tau in the presence of 10-fold excess MB (Figure 4a), though the variability of the data in this experiment was particularly high ($p = .70$). The dimer abundance of the other five isoforms was not affected by the presence of MB. Similar data were observed in IM-MS analysis (Figure 4b), which supported a ~ 3 -fold increase in dimer abundance of 0N3R-tau in the presence of MB, and in this case, the difference was statistically significant.

3 | DISCUSSION

Despite a large body of research on tau structure and aggregation, the initial oligomerization of the six isoforms of tau in their unmodified form has not been studied

systematically to date. Here, we attempted to close this knowledge gap by applying several biochemical and biophysical methods to the characterization of the oligomers formed by each tau isoform, in the absence of modifiers or posttranslational modifications, both in solution and when the protein is transferred into the gas phase under gentle conditions that allow studying oligomers.^{74,75} The main finding of our study is that under the conditions we used, 3R- and 4R-tau isoforms form different oligomer size distributions. Our goal was to characterize oligomers in unmodified, unmanipulated human tau, which is not known to aggregate *in vitro* in the absence of inducers,⁶⁸ to form oligomers in the absence of oligomerization seeds,³⁵ or to cause toxicity to cultured cells. In fact, unmodified monomeric tau has been used as a negative control in experiments examining the toxicity of tau oligomers seeded using A β or α -synuclein oligomers.⁷⁶ As we did not use such inducers, we limited the investigation to comparing the initial oligomer size distributions and antibody reactivity of each isoform and did not attempt to characterize their toxicity.

Dot-blot analysis showed that 3R-tau isoforms have a higher propensity to form TOC1-immunoreactive oligomers compared to 4R tau isoforms (Figure 1). Previous reports have suggested that TOC1 mainly reacts with tau dimers,³⁶ yet we did not observe reactivity of TOC1 with any oligomers when the different tau isoforms were

fractionated by native-PAGE (Figure S1), possibly due to loss of the epitope under the assay conditions. However, probing the same membranes with the anti-human-tau mAb HT7 showed that indeed the dimer abundance of 3R-tau isoforms was higher than in 4R-isoforms. Interestingly, the one exception was 0N4R-tau, whose TOC1 reactivity was similar to that of 3R isoforms. This isoform was found by the MS (Figure 4a) and IM-MS (Figure 4b) experiments to form substantially more abundant dimers than all other isoforms, providing a possible explanation for its high TOC1 reactivity.

The higher reactivity of TOC1 with 3R-tau isoforms also correlated with formation of HMW oligomers in our PICUP experiments (Figure 3), which were substantially more abundant than in 4R-tau isoforms, suggesting that they may form by self-association of dimers. This hypothesis is supported by a previous study suggesting that tau dimers may nucleate formation of higher order oligomers.³⁶ The PICUP data also supported particular stabilization of dimers of 0N4R-tau (Figure 3c) compared to other isoforms, in agreement with the MS and IM-MS data. Such stabilization was not observed in the native-PAGE/western blot analysis (Figure 2), possibly due to the different assay conditions.

These data suggest that oligomer formation tendencies of the different tau isoforms are dictated primarily by the absence or presence of the second repeat in the microtubule-binding domain, which is absent in 3R-tau. Our findings correlate with observations that 3R segments are part of the ordered core of tau fibrils in 3R, 4R, and 3R + 4R tauopathies, including AD, CBD, CTE, and Pick's fibril cores.⁷⁷⁻⁸² However, our study points to a key role of the repeat-domain not only in the final fibril structure, but also in the initial oligomerization.

Immunohistochemistry studies of postmortem AD brain sections using specific monoclonal antibodies for 3R-tau and 4R-tau have shown higher distribution of 3R-tau in the majority of the NFTs in the hippocampus and cortex.⁸³ The study suggested that the higher contribution of 3R-tau isoforms to NFTs correlated better with pathology progression 4R-tau isoforms. In another study, the sarkosyl-insoluble fractions of postmortem AD brains showed higher amounts of 3R- compared to 4R-tau.⁸⁴ A *Drosophila* model of tauopathy also showed a higher contribution of accumulated 0N3R-tau in disrupting signal transduction compared to 0N4R.¹⁷ Our results are consistent with these studies and suggest that the pathological effects of 3R-tau may be related to a higher propensity of unmodified 3R-tau isoforms to form dimers and HMW oligomers than 4R-tau isoforms.

In agreement with our previous examination of tau seeding in cell culture, which showed that the addition of DTT had little effect on the seeding capability of different

forms of tau,⁶⁸ here we found that adding DTT did not affect meaningfully the oligomerization of any of the tau isoforms (Figure 2b), possibly because the proteins were reduced in the process of their purification. Nonetheless, these data suggest that the higher tendency of 3R-tau isoforms to form dimers and HMW oligomers we observed was not simply controlled by disulfide bond formation.

Our study supports a growing body of evidence for the importance of oligomeric tau, rather than the insoluble aggregates, for the disease-related neuronal dysfunction and death in tauopathies.^{47,85} We find that oligomerization is a natural tendency of tau, even in the absence of posttranslational modifications, seeds, or assembly inducers. Moreover, we find that 0N and 1N isoforms are more susceptible to oligomerization than 2N isoforms. The native-PAGE analysis showed that 1N3R-tau has the highest dimer abundance among all the tau isoforms and 1N4R-tau and 0N4R-tau displayed slightly higher dimer abundance compared to 2N4R-tau. The PICUP study suggests that the presence or absence of the two N-terminal inserts in 4R-tau isoforms has substantial effects on the oligomer size distributions of 4R-tau isoforms. These data suggest that the contribution of exons 2 and 3-coded sequences is important in tau oligomerization and deserves more attention in further studies.

MB has been reported to decrease tau oligomerization and aggregation in different tauopathy models.⁸⁶⁻⁸⁸ A phase 2 clinical trial of MB in mild/moderate patients with AD showed significant cognitive improvement, yet in a follow-up phase 3 trials, MB failed to meet the primary outcomes,^{89,90} possibly because it did not affect tau oligomers.⁶⁵ Here, we tested the effect of MB on the six tau isoforms' oligomerization and found conflicting results. The compound appeared to reduce tau oligomers of only 3R isoforms in dot blots probed with TOC1 (Figure 5), but native-PAGE analysis did not show a change in oligomers of any isoform (Figure S3) and IM-MS data suggested an increase in 0N3R-tau oligomers (Figure 4b). Taken together, these inconclusive data support the notion that MB does not have a substantial impact on the tau oligomers studied here.

The molecular tweezer, CLR01, has been developed by our group and shown to inhibit aggregation of multiple amyloidogenic proteins,^{91,92} including 0N3R tau induced to aggregate by arachidonic acid⁶⁷ and 2N4R tau induced to aggregate by heparin or phosphorylated *in vitro*.⁶⁸ It also was shown to inhibit seeded intracellular tau aggregation and reduce tau oligomers and seeds in transgenic mouse brains.⁶² The lack of an effect of CLR01 on the tau oligomers studied here suggests that they are distinct from those found *in vivo*, as might be

expected. Similarly, we did not find any modulation activity for the all τ -peptide, D-TLKIVW, a specific tau aggregation-inhibitor that has been shown to prevent fibrillation of tau fragments,⁷¹ possibly because those fragments are distinct from the full-length tau proteins studied here and/or because the peptide might inhibit only fibril elongation but not the initial oligomerization of tau.

In conclusion, our study provides new insight into the extent to which the structural elements that distinguish the six human tau isoforms, the N-terminal inserts encoded by exons 2 and 3, and the second repeat encoded by exon 10, control tau oligomerization. The data suggest that the absence of the second repeat promotes initial oligomerization, whereas the N-terminal inserts have more subtle, yet significant effects on the initial tau oligomerization. This information is important for analyzing the seeding capacity and cytotoxicity of tau and will serve as a baseline for future analysis of posttranslationally modified forms of tau toward an improved mechanistic understanding of the forces driving the self-assembly of the protein into neurotoxic oligomers and aggregates.

4 | MATERIALS AND METHODS

4.1 | Expression and purification of recombinant tau

Plasmids encoding the six wild-type human tau isoforms were a generous gift from Dr. Stuart Feinstein (University of California Santa Barbara). All plasmids contained DNA encoding a N-terminal $6 \times$ His tag for purification. Expression and purification of each isoform were similar to those described previously.⁹³ Briefly, tau was expressed in BL21 (DE3) bacteria (Invitrogen, Waltham, MA). Bacterial cells were lysed using a high-pressure EMULSIFLEX homogenizer (Avestin, Mannheim, Germany) and the lysates were heated for 15 min at 95°C and filtered. The filtrates were loaded onto a Ni-NTA affinity-chromatography column (HisTrap HP, GE Healthcare, Chicago, IL). Tau-containing fractions were detected using SDS-PAGE followed by Coomassie Brilliant Blue staining, pooled, and incubated overnight with tobacco-etch virus (TEV) protease to cleave the $6 \times$ His tag. The reaction mixture was loaded onto a Ni-NTA column, and the tag-free tau was collected in the flow-through and dialyzed against an ion-exchange buffer comprising 50 mM MES, 50 mM NaCl, and 1 mM dithiothreitol (DTT), pH 6.8. The protein solution was fractionated using a NaCl gradient from 50 to 150 mM on an ion-exchange chromatography column (HiTrap SP HP, GE Healthcare) and tau-containing fractions were

pooled. Finally, the protein was purified further by size-exclusion chromatography using a S200 column (GE Healthcare) and $1 \times$ phosphate-buffered saline (PBS) as the mobile phase. Fractions containing purified tau were pooled and concentrated by ultrafiltration (Amicon® Ultra 15, Millipore Sigma, 10 kDa molecular-weight cutoff). The protein concentration and purity were determined by a bicinchoninic acid (BCA) assay and densitometric analysis, respectively. The yield was in the range of 1–8 mg starting with a 3 L culture volume and the purity was >90%. The purified protein was aliquoted and stored at -80°C until the time of use.

4.2 | Dot blot analysis

Five hundred nanograms of each tau isoform were spotted onto 0.22- μm nitrocellulose membranes (Thermo Fisher Scientific, Waltham, MA). Membranes were blocked in blocking buffer comprising 5% non-fat dry milk powder in Tris-buffered saline containing 0.1% Tween-20 (TBST) for 1 hr at room temperature (RT) and then incubated with antibody TOC-1 (1:5,000 dilution), stripped, and re-probed with antibody HT7 (1:1,000). Membranes were washed thrice for 10 min in TBST followed by incubation with horseradish peroxidase (HRP)-conjugated goat anti-mouse antibody for 1 hr at RT. The membranes were developed using SuperSignal West Pico PLUS Chemiluminescent Substrate (Life Technologies, Carlsbad, CA) and visualized using an Azure Biosystems c300 Gel Imager.

4.3 | Native-PAGE/western blot

Each tau isoform was fractionated using Novex NativePAGE 3–12% gradient Bis-Tris gels (Thermo Fisher Scientific) as described previously.⁹⁴ Briefly, tau samples were prepared by mixing the protein solution with a Native-PAGE sample buffer comprising 50 mM bis-Tris, 10 mM NaCl, 12% glycerol, and 0.001% Ponceau S, pH 7.2, on ice, and 500 ng of each sample were loaded on the gels. Following the gel run, the proteins were transferred onto polyvinylidene difluoride (PVDF) membranes (Thermo Fisher Scientific) for 1 hr at 25 V on ice using XCell II Blot Modules (Invitrogen). Proteins then were fixed in 8% acetic acid for 15 min and the membranes were air dried. Membranes were reactivated in methanol and blocked in 5% non-fat dry milk in TBST for 1 hr at RT. The membranes were probed with TOC1 (1:5,000 dilution), stripped, and re-probed with HT7 (1:1,000). Membranes were washed and incubated with HRP-conjugated goat anti-mouse antibody (Thermo Fisher

Scientific) at 1:10,000 dilution in blocking buffer for 1 hr at RT, developed using SuperSignal West Pico PLUS Chemiluminescent Substrate (Life Technologies), and visualized using an Azure Biosystems c300 Gel Imager.^{95,96}

4.4 | PICUP and SDS-PAGE analysis

Each tau isoform was cross-linked using PICUP⁴⁵ as described previously.^{46,97} In brief, 1 μ l of 40 μ M Tris (2,2-bipyridyl)-dichlororuthenium (II) hexahydrate [Ru (Bpy)] and 1 μ l of 800 μ M ammonium persulfate, prepared in PBS were added to 18 μ l of 10 μ M of tau (protein to Ru(Bpy) molar ratio 1:4). The mixture was vortexed briefly and irradiated for 1 s using a 150 W visible light source (model 170-D, Dolan-Jenner, Lawrence, MA), after which the free-radical reaction was quenched by adding 1 μ l of 1 M DTT (Thermo Fisher Scientific) in PBS, followed by brief vortexing. Cross-linked proteins were mixed with 4 \times LDS NuPAGE sample buffer (Invitrogen), heated at 95°C for 5 min, and 250 ng of each protein mixture was fractionated by SDS-PAGE using 4–12% bis-Tris gradient gels (GenScript). Non-cross-linked proteins were used as negative controls in each case. The proteins were visualized by silver staining (SilverXpress, Invitrogen).

4.5 | Inhibitor analysis

Tau isoforms were mixed with each inhibitor at a 1:10 concentration ratio, respectively. Inhibitors were prepared at a stock concentration of 2 mM in 1 \times PBS and 1 μ l of the stock was added to 10 μ M protein. Dot blot and Native-PAGE analyses were performed immediately after adding the inhibitors to the protein, as described above. For mass spectrometry experiments, tau isoforms were diluted to 10 μ M and sprayed in 20 mM ammonium acetate. Methylene blue was added at a 10 \times concentration into the solution of tau.

4.6 | Mass spectrometry

The samples in the absence or presence of inhibitors were loaded into custom gold-coated borosilicate capillaries. The samples were sprayed at a capillary voltage of 1.5 kV on a Waters Synapt G2 Si mass spectrometer in time-of-flight (TOF) mode. Scans were collected over 2 min using a scan time of 1 s. Three to five replicates were collected for each sample. The TOF data were deconvoluted using UniDec,⁹⁸ and the deconvoluted dimer and monomer intensities were quantified.

Ion-mobility analysis was performed by spraying the samples in Mobility TOF mode. The wave velocity was set at 1,000 m/s. These experiments were collected over 5 min using a scan time of 1 s. The scans from 14.38 to 21.98 ms were extracted for the maximum intensity of the dimers. Three to five replicates were collected for each sample. The spectrum extracted from the mobiligram range was deconvoluted with UniDec and the deconvoluted dimer and monomer intensities were compared.

4.7 | Statistics

Statistical analysis was performed using GraphPad Prism 9.2. Data are shown as mean \pm SD for a minimum of three independent experiments and three technical replicates in each case.

ACKNOWLEDGMENTS

We thank Dr Stuart Feinstein, University of California Santa Barbara, for the kind gift of the tau plasmids, Nick Kanaan, Michigan State University for the generous gift of antibody TOC1, and Dr David Eisenberg, University of California Los Angeles for the use of his chromatography systems. The study was supported by NIH/NIA grants R01AG050721 and RF1AG054000 (Gal Bitan), an Administrative Supplement to Promote Diversity RF1AG054000-01A1S1 (to Jennifer Portillo), NIH R01GM103479 and S10 OD018504 (Joseph A. Loo), the US Department of Energy DE-FC02-02ER63421 (Joseph A. Loo), and a Ruth L. Kirschstein National Research Service Award program GM007185 (Carter Lantz).

CONFLICT OF INTEREST

The authors declare no conflicts of interest.

AUTHOR CONTRIBUTIONS

Hedieh Shahpasand-Kroner: Data curation (lead); formal analysis (equal); investigation (lead); supervision (supporting); writing – original draft (lead). **Jennifer Portillo:** Data curation (supporting); resources (lead). **Carter Lantz:** Data curation (equal); formal analysis (equal); investigation (equal); writing – original draft (supporting). **Paul M. Seidler:** Data curation (supporting); investigation (supporting); writing – review and editing (supporting). **Natalie Sarafian:** Resources (supporting). **Joseph A. Loo:** Formal analysis (equal); funding acquisition (supporting); methodology (equal); project administration (supporting); supervision (supporting); writing – review and editing (supporting). **Gal Bitan:** Conceptualization (lead); data curation (equal); formal analysis (equal); funding acquisition

(lead); project administration (lead); supervision (lead); writing – review and editing (lead).

ORCID

Gal Bitan  <https://orcid.org/0000-0001-7046-3754>

REFERENCES

1. Andreadis A, Brown W, Kosik K. Structure and novel exons of the human *t* gene. *Biochemistry*. 1992;31:10626–10633.
2. Goedert M, Spillantini MG. Tau gene mutations and neurodegeneration. *Biochem Soc Symp*. 2001;67:59–71.
3. Goedert M, Spillantini MG, Jakes R, Rutherford D, Crowther RA. Multiple isoforms of human microtubule-associated protein tau: Sequences and localization in neurofibrillary tangles of Alzheimer's disease. *Neuron*. 1989;3(4):519–526.
4. LoPresti P, Szuchet S, Papasozomenos SC, Zinkowski RP, Binder LI. Functional implications for the microtubule-associated protein tau: Localization in oligodendrocytes. *Proc Natl Acad Sci USA*. 1995;92(22):10369–10373.
5. Müller R, Heinrich M, Heck S, Blohm D, Richter-Landsberg C. Expression of microtubule-associated proteins MAP2 and tau in cultured rat brain oligodendrocytes. *Cell Tissue Res*. 1997;288(2):239–249.
6. Cleveland D, Hwo S, Kirschner M. Physical and chemical properties of purified tau factor and the role of tau in microtubule assembly. *J Mol Biol*. 1977;116:227–247.
7. Arendt T, Stieler JT, Holzer M. Tau and tauopathies. *Brain Res Bull*. 2016;126(Pt 3):238–292.
8. Medina M, Hernandez F, Avila J. New features about tau function and dysfunction. *Biomolecules*. 2016;6(2):21.
9. Trabzuni D, Wray S, Vandrovicova J, et al. MAPT expression and splicing is differentially regulated by brain region: Relation to genotype and implication for tauopathies. *Hum Mol Genet*. 2012;21(18):4094–4103.
10. Stoothoff W, Jones PB, Spires-Jones TL, et al. Differential effect of three-repeat and four-repeat tau on mitochondrial axonal transport. *J Neurochem*. 2009;111(2):417–427.
11. Boyne LJ, Tessler A, Murray M, Fischer I. Distribution of big tau in the central nervous system of the adult and developing rat. *J Comp Neurol*. 1995;358(2):279–293.
12. Lee VM, Goedert M, Trojanowski JQ. Neurodegenerative tauopathies. *Annu Rev Neurosci*. 2001;24:1121–1159.
13. Lee VM, Trojanowski JQ. Neurodegenerative tauopathies: Human disease and transgenic mouse models. *Neuron*. 1999;24(3):507–510.
14. Spillantini MG, Goedert M. Tau protein pathology in neurodegenerative diseases [review]. *Trends Neurosci*. 1998;21(10):428–433.
15. Kovacs GG. Invited review: Neuropathology of tauopathies: Principles and practice. *Neuropathol Appl Neurobiol*. 2015;41(1):3–23.
16. McKee AC, Stein TD, Nowinski CJ, et al. The spectrum of disease in chronic traumatic encephalopathy. *Brain*. 2013;136(Pt 1):43–64.
17. Kadas D, Papanikolopoulou K, Xirou S, Consoulas C, Skoulakis EMC. Human tau isoform-specific presynaptic deficits in a drosophila central nervous system circuit. *Neurobiol Dis*. 2019;124:311–321.
18. Sealey MA, Vourkou E, Cowan CM, et al. Distinct phenotypes of three-repeat and four-repeat human tau in a transgenic model of tauopathy. *Neurobiol Dis*. 2017;105:74–83.
19. King ME, Gamblin TC, Kuret J, Binder LI. Differential assembly of human tau isoforms in the presence of arachidonic acid. *J Neurochem*. 2000;74(4):1749–1757.
20. Zhang W, Falcon B, Murzin AG, et al. Heparin-induced tau filaments are polymorphic and differ from those in Alzheimer's and Pick's diseases. *Elife*. 2019;8:e43584.
21. Despres C, Byrne C, Qi H, et al. Identification of the tau phosphorylation pattern that drives its aggregation. *Proc Natl Acad Sci USA*. 2017;114(34):9080–9085.
22. Maeda S, Sahara N, Saito Y, Murayama S, Ikai A, Takashima A. Increased levels of granular tau oligomers: An early sign of brain aging and Alzheimer's disease. *Neurosci Res*. 2006;54(3):197–201.
23. Santacruz K, Lewis J, Spires T, et al. Tau suppression in a neurodegenerative mouse model improves memory function. *Science*. 2005;309(5733):476–481.
24. Berger Z, Roder H, Hanna A, et al. Accumulation of pathological tau species and memory loss in a conditional model of tauopathy. *J Neurosci*. 2007;27(14):3650–3662.
25. Lasagna-Reeves CA, Castillo-Carranza DL, Sengupta U, Clos AL, Jackson GR, Kaye R. Tau oligomers impair memory and induce synaptic and mitochondrial dysfunction in wild-type mice. *Mol Neurodegener*. 2011;6:39.
26. Sydow A, van der Jeugd A, Zheng F, et al. Tau-induced defects in synaptic plasticity, learning, and memory are reversible in transgenic mice after switching off the toxic tau mutant. *J Neurosci*. 2011;31(7):2511–2525.
27. Lasagna-Reeves CA, Castillo-Carranza DL, Sengupta U, et al. Identification of oligomers at early stages of tau aggregation in Alzheimer's disease. *FASEB J*. 2012;26(5):1946–1959.
28. Ghag G, Bhatt N, Cantu DV, et al. Soluble tau aggregates, not large fibrils, are the toxic species that display seeding and cross-seeding behavior. *Protein Sci*. 2018;27(11):1901–1909.
29. Tiernan CT, Mufson EJ, Kanaan NM, Counts SE. Tau oligomer pathology in nucleus Basalis neurons during the progression of Alzheimer disease. *J Neuropathol Exp Neurol*. 2018;77(3):246–259.
30. Lo CH, Lim CKW, Ding Z, et al. Targeting the ensemble of heterogeneous tau oligomers in cells: A novel small molecule screening platform for tauopathies. *Alzheimers Dement*. 2019;15(11):1489–1502.
31. Andorfer C, Acker CM, Kress Y, Hof PR, Duff K, Davies P. Cell-cycle reentry and cell death in transgenic mice expressing nonmutant human tau isoforms. *J Neurosci*. 2005;25(22):5446–5454.
32. Polydoro M, Acker CM, Duff K, Castillo PE, Davies P. Age-dependent impairment of cognitive and synaptic function in the htau mouse model of tau pathology. *J Neurosci*. 2009;29(34):10741–10749.
33. Ishihara T, Zhang B, Higuchi M, Yoshiyama Y, Trojanowski JQ, Lee VMY. Age-dependent induction of congophilic neurofibrillary tau inclusions in tau transgenic mice. *Am J Pathol*. 2001;158(2):555–562.
34. Spires TL, Orne JD, SantaCruz K, et al. Region-specific dissociation of neuronal loss and neurofibrillary pathology in a mouse model of tauopathy. *Am J Pathol*. 2006;168(5):1598–1607.

35. Lasagna-Reeves CA, Castillo-Carranza DL, Guerrero-Muñoz MJ, Jackson GR, Kaye R. Preparation and characterization of neurotoxic tau oligomers. *Biochemistry*. 2010;49(47):10039–10041.
36. Patterson KR, Remmers C, Fu Y, et al. Characterization of pre-fibrillar tau oligomers in vitro and in Alzheimer disease. *J Biol Chem*. 2011;286(26):23063–23076.
37. Castillo-Carranza DL, Sengupta U, Guerrero-Munoz MJ, et al. Passive immunization with tau oligomer monoclonal antibody reverses tauopathy phenotypes without affecting hyperphosphorylated neurofibrillary tangles. *J Neurosci*. 2014;34(12):4260–4272.
38. Castillo-Carranza DL, Gerson JE, Sengupta U, Guerrero-Muñoz MJ, Lasagna-Reeves CA, Kaye R. Specific targeting of tau oligomers in Htau mice prevents cognitive impairment and tau toxicity following injection with brain-derived tau oligomeric seeds. *J Alzheimers Dis*. 2014;40(Suppl 1):S97–S111.
39. Goedert M, Jakes R. Expression of separate isoforms of human tau protein: Correlation with the tau pattern in brain and effects on tubulin polymerization. *EMBO J*. 1990;9(13):4225–4230.
40. Sahara N, Maeda S, Murayama M, et al. Assembly of two distinct dimers and higher-order oligomers from full-length tau. *Eur J Neurosci*. 2007;25(10):3020–3029.
41. Bitan G, Teplow DB. Rapid photochemical cross-linking—A new tool for studies of metastable, amyloidogenic protein assemblies. *Acc Chem Res*. 2004;37(6):357–364.
42. Bitan G, Lomakin A, Teplow DB. Amyloid β -protein oligomerization: Prenucleation interactions revealed by photo-induced cross-linking of unmodified proteins. *J Biol Chem*. 2001;276(37):35176–35184.
43. Acharya S, Safaie BM, Wongkongkathep P, et al. Molecular basis for preventing α -synuclein aggregation by a molecular tweezer. *J Biol Chem*. 2014;289(15):10727–10737.
44. Lopes DH, Sinha S, Rosensweig C, Bitan G. Application of photochemical cross-linking to the study of oligomerization of amyloidogenic proteins. *Methods Mol Biol*. 2012;849:11–21.
45. Fancy DA, Kodadek T. Chemistry for the analysis of protein-protein interactions: Rapid and efficient cross-linking triggered by long wavelength light. *Proc Natl Acad Sci USA*. 1999;96(11):6020–6024.
46. Bitan G. Structural study of metastable amyloidogenic protein oligomers by photo-induced cross-linking of unmodified proteins. *Methods Enzymol*. 2006;413:217–236.
47. Bernstein SL, Dupuis NF, Lazo ND, et al. Amyloid- β protein oligomerization and the importance of tetramers and dodecamers in the aetiology of Alzheimer's disease. *Nat Chem*. 2009;1(4):326–331.
48. Bernstein SL, Wyttenbach T, Baumketner A, et al. Amyloid β -protein: Monomer structure and early aggregation states of A β 42 and its Pro19 alloform. *J Am Chem Soc*. 2005;127(7):2075–2084.
49. Nshanian M, Lantz C, Wongkongkathep P, et al. Native top-down mass spectrometry and ion mobility spectrometry of the interaction of tau protein with a molecular Tweezer assembly modulator. *J Am Soc Mass Spectrom*. 2019;30(1):16–23.
50. Wongkongkathep P, Han JY, Choi TS, Yin S, Kim HI, Loo JA. Native top-down mass spectrometry and ion mobility MS for characterizing the cobalt and manganese metal binding of alpha-Synuclein protein. *J Am Soc Mass Spectrom*. 2018;29(9):1870–1880.
51. Arya S, Claud SL, Cantrell KL, Bowers MT. Catalytic prion-like cross-talk between a key Alzheimer's disease tau-fragment R3 and the type 2 diabetes peptide IAPP. *ACS Chem Neurosci*. 2019;10(11):4757–4765.
52. Feinstein HE, Benbow SJ, LaPointe NE, et al. Oligomerization of the microtubule-associated protein tau is mediated by its N-terminal sequences: Implications for normal and pathological tau action. *J Neurochem*. 2016;137(6):939–954.
53. Eschmann NA, Do TD, LaPointe NE, et al. Tau aggregation propensity engrained in its solution state. *J Phys Chem B*. 2015;119(45):14421–14432.
54. Do TD, Economou NJ, Chamas A, Buratto SK, Shea JE, Bowers MT. Interactions between amyloid-beta and tau fragments promote aberrant aggregates: Implications for amyloid toxicity. *J Phys Chem B*. 2014;118(38):11220–11230.
55. Ganguly P, Do TD, Larini L, et al. Tau assembly: The dominant role of PHF6 (VQIVYK) in microtubule binding region repeat R3. *J Phys Chem B*. 2015;119(13):4582–4593.
56. Larini L, Gessel MM, LaPointe NE, et al. Initiation of assembly of tau(273-284) and its DeltaK280 mutant: An experimental and computational study. *Phys Chem Chem Phys*. 2013;15(23):8916–8928.
57. Ahmadi S, Zhu S, Sharma R, Wilson DJ, Kraatz HB. Interaction of metal ions with tau protein. The case for a metal-mediated tau aggregation. *J Inorg Biochem*. 2019;194:44–51.
58. Jebarupa B, Muralidharan M, Arun A, Mandal AK, Mitra G. Conformational heterogeneity of tau: Implication on intrinsic disorder, acid stability and fibrillation in Alzheimer's disease. *Biophys Chem*. 2018;241:27–37.
59. Jebarupa B, Muralidharan M, Srinivasu BY, Mandal AK, Mitra G. Effect of altered solution conditions on tau conformational dynamics: Plausible implication on order propensity and aggregation. *Biochim Biophys Acta Proteins Proteomics*. 2018;1866(5–6):668–679.
60. Hochgrafe K, Sydow A, Matenia D, et al. Preventive methylene blue treatment preserves cognition in mice expressing full-length pro-aggregant human tau. *Acta Neuropathol Commun*. 2015;3:25.
61. Gerson J, Kaye R. Therapeutic approaches targeting pathological tau aggregates. *Curr Pharm Des*. 2016;22(26):4028–4039.
62. Di J, Siddique I, Li Z, et al. The molecular tweezer CLR01 improves behavioral deficits and reduces tau pathology in P301S-tau transgenic mice. *Alzheimers Res Ther*. 2021;13(1):6.
63. Seidler PM, Boyer DR, Murray KA, et al. Structure-based inhibitors halt prion-like seeding by Alzheimer's disease-and tauopathy-derived brain tissue samples. *J Biol Chem*. 2019;294(44):16451–16464.
64. Wischik CM, Edwards PC, Lai RY, Roth M, Harrington CR. Selective inhibition of Alzheimer disease-like tau aggregation by phenothiazines. *Proc Natl Acad Sci USA*. 1996;93(20):11213–11218.
65. Soeda Y, Saito M, Maeda S, et al. Methylene blue inhibits formation of tau fibrils but not of granular tau oligomers: A plausible key to understanding failure of a clinical trial for Alzheimer's disease. *J Alzheimers Dis*. 2019;68(4):1677–1686.
66. Busche MA, Hyman BT. Synergy between amyloid- β and tau in Alzheimer's disease. *Nat Neurosci*. 2020;23(10):1183–1193.

67. Sinha S, Lopes DHJ, du Z, et al. Lysine-specific molecular tweezers are broad-spectrum inhibitors of assembly and toxicity of amyloid proteins. *J Am Chem Soc.* 2011;133(42):16958–16969.
68. Despres C, Di J, Cantrelle FX, et al. Major differences between the self-assembly and seeding behavior of heparin-induced and in vitro phosphorylated tau and their modulation by potential inhibitors. *ACS Chem Biol.* 2019;14(6):1363–1379.
69. Sinha S, Du Z, Maiti P, et al. Comparison of three amyloid assembly inhibitors: The sugar scyllo-inositol, the polyphenol epigallocatechin gallate, and the molecular tweezer CLR01. *ACS Chem Neurosci.* 2012;3(6):451–458.
70. Attar A, Ripoli C, Riccardi E, et al. Protection of primary neurons and mouse brain from Alzheimer's pathology by molecular tweezers. *Brain.* 2012;135(Pt 12):3735–3748.
71. Sievers SA, Karanicolas J, Chang HW, et al. Structure-based design of non-natural amino-acid inhibitors of amyloid fibril formation. *Nature.* 2011;475(7354):96–100.
72. Zheng J, Liu C, Sawaya MR, et al. Macrocyclic beta-sheet peptides that inhibit the aggregation of a tau-protein-derived hexapeptide. *J Am Chem Soc.* 2011;133(9):3144–3157.
73. Li Z, Siddique I, Hadrović I, et al. Lysine-selective molecular tweezers are cell penetrant and concentrate in lysosomes. *Commun Biol.* 2021;4(1):1076.
74. Teplow DB, Lazo ND, Bitan G, et al. Elucidating amyloid β -protein folding and assembly: A multidisciplinary approach. *Acc Chem Res.* 2006;39(9):635–645.
75. Hoffmann W, von Helden G, Pagel K. Ion mobility-mass spectrometry and orthogonal gas-phase techniques to study amyloid formation and inhibition. *Curr Opin Struct Biol.* 2017;46:7–15.
76. Flach K, Hilbrich I, Schiffmann A, et al. Tau oligomers impair artificial membrane integrity and cellular viability. *J Biol Chem.* 2012;287(52):43223–43233.
77. Fitzpatrick AWP, Falcon B, He S, et al. Cryo-EM structures of tau filaments from Alzheimer's disease. *Nature.* 2017;547(7662):185–190.
78. Falcon B, Zhang W, Schweighauser M, et al. Tau filaments from multiple cases of sporadic and inherited Alzheimer's disease adopt a common fold. *Acta Neuropathol.* 2018;136(5):699–708.
79. Falcon B, Zhang W, Murzin AG, et al. Structures of filaments from Pick's disease reveal a novel tau protein fold. *Nature.* 2018;561(7721):137–140.
80. Falcon B, Zivanov J, Zhang W, et al. Novel tau filament fold in chronic traumatic encephalopathy encloses hydrophobic molecules. *Nature.* 2019;568(7752):420–423.
81. Zhang W, Tarutani A, Newell KL, et al. Novel tau filament fold in corticobasal degeneration. *Nature.* 2020;580(7802):283–287.
82. Shi Y, Zhang W, Yang Y, et al. Structure-based classification of tauopathies. *Nature.* 2021;598:359–363.
83. Espinoza M, de Silva R, Dickson DW, Davies P. Differential incorporation of tau isoforms in Alzheimer's disease. *J Alzheimers Dis.* 2008;14(1):1–16.
84. Liu WK, Le TV, Adamson J, et al. Relationship of the extended tau haplotype to tau biochemistry and neuropathology in progressive supranuclear palsy. *Ann Neurol.* 2001;50(4):494–502.
85. Lasagna-Reeves CA, Castillo-Carranza DL, Sengupta U, et al. Alzheimer brain-derived tau oligomers propagate pathology from endogenous tau. *Sci Rep.* 2012;2:700.
86. Fatouros C, Pir GJ, Biernat J, et al. Inhibition of tau aggregation in a novel *Caenorhabditis elegans* model of tauopathy mitigates proteotoxicity. *Hum Mol Genet.* 2012;21(16):3587–3603.
87. Hosokawa M, Arai T, Masuda-Suzukake M, et al. Methylene blue reduced abnormal tau accumulation in P301L tau transgenic mice. *PLoS One.* 2012;7(12):e52389.
88. Spires-Jones TL, Friedman T, Pitstick R, et al. Methylene blue does not reverse existing neurofibrillary tangle pathology in the rTg4510 mouse model of tauopathy. *Neurosci Lett.* 2014;562:63–68.
89. Wilcock GK, Gauthier S, Frisoni GB, et al. Potential of low dose leuco-methylthionium bis(hydromethanesulphonate) (LMTM) monotherapy for treatment of mild Alzheimer's disease: Cohort analysis as modified primary outcome in a phase III clinical trial. *J Alzheimers Dis.* 2018;61(1):435–457.
90. Gauthier S, Feldman HH, Schneider LS, et al. Efficacy and safety of tau-aggregation inhibitor therapy in patients with mild or moderate Alzheimer's disease: A randomised, controlled, double-blind, parallel-arm, phase 3 trial. *Lancet.* 2016;388(10062):2873–2884.
91. Attar A, Bitan G. Disrupting self-assembly and toxicity of amyloidogenic protein oligomers by “molecular tweezers”—From the test tube to animal models. *Curr Pharm Des.* 2014;20(15):2469–2483.
92. Schrader T, Bitan G, Klärner FG. Molecular tweezers for lysine and arginine—Powerful inhibitors of pathologic protein aggregation. *Chem Commun (Camb).* 2016;52(76):11318–11334.
93. Best RL, Chung PJ, Benbow SJ, et al. Expression and isolation of recombinant tau. *Methods Cell Biol.* 2017;141:3–26.
94. Herrera-Vaquero M, Bouquio D, Kallab M, et al. The molecular tweezer CLR01 reduces aggregated, pathologic, and seeding-competent α -synuclein in experimental multiple system atrophy. *Biochim Biophys Acta Mol Basis Dis.* 2019;1865(11):165513.
95. Abramoff MD, Magelhaes PJ, Ram SJ. Image processing with ImageJ. *Biophotonics Int.* 2004;11(7):36–42.
96. Schneider CA, Rasband WS, Eliceiri KW. NIH image to ImageJ: 25 years of image analysis. *Nat Methods.* 2012;9(7):671–675.
97. Rahimi F, Maiti P, Bitan G. Photo-induced cross-linking of unmodified proteins (PICUP) applied to amyloidogenic peptides. *J Vis Exp.* 2009;23:1071.
98. Marty MT, Baldwin AJ, Marklund EG, Hochberg GKA, Benesch JLP, Robinson CV. Bayesian deconvolution of mass and ion mobility spectra: From binary interactions to polydisperse ensembles. *Anal Chem.* 2015;87(8):4370–4376.

SUPPORTING INFORMATION

Additional supporting information may be found in the online version of the article at the publisher's website.

How to cite this article: Shahpasand-Kroner H, Portillo J, Lantz C, Seidler PM, Sarafian N, Loo JA, et al. Three-repeat and four-repeat tau isoforms form different oligomers. *Protein Science.* 2022;31:613–27. <https://doi.org/10.1002/pro.4257>